

## Self-Assembly Mechanism of a Bimetallic Europium Triple-Stranded Helicate

Josef Hamacek,<sup>†</sup> Sylvie Blanc,<sup>†</sup> Mourad Elhabiri,<sup>†</sup> Emmanuelle Leize,<sup>§</sup>  
Alain Van Dorsselaer,<sup>§</sup> Claude Piguet,<sup>‡</sup> and Anne-Marie Albrecht-Gary<sup>\*†</sup>

Contribution from the Laboratoire de Physico-Chimie Bioinorganique, UMR 7509 du CNRS, ECPM, Université Louis Pasteur, 25 rue Becquerel, 67200 Strasbourg, France, the Laboratoire de Spectrométrie de Masse Bioorganique, UMR 7509 du CNRS, ECPM, Université Louis Pasteur, 25 rue Becquerel, 67200 Strasbourg, France and the Department of Inorganic, Analytical and Applied Chemistry, University of Geneva, CH-1211 Geneva 4, Switzerland

Received October 8, 2002; E-mail: amalbre@chimie.u-strasbg.fr

**Abstract:** We report the self-assembly process of a supramolecular edifice based on the coordination of europium(III) by a ditopic strand **L** bearing tridentate bis(benzimidazolyl)pyridine subunits. Varying the metal/ligand ratio and using a fruitful combination of electrospray mass spectrometry and absorption spectrophotometry, we characterized three major complexes ( $\text{EuL}_2$ ,  $\text{Eu}_2\text{L}_2$ , and  $\text{Eu}_2\text{L}_3$ ) in acetonitrile. Kinetic investigations showed an alternative “braiding” and “keystone” mechanism leading to  $\text{Eu}_2\text{L}_3$ . The formation mechanism of the dinuclear triple-stranded helicate, which is mainly governed by electrostatic interactions, goes via the “side-by-side”  $\text{Eu}_2\text{L}_2$  intermediate. Our thermodynamic and kinetic data allow the prediction of the apparent “magic” self-assembly of  $\text{Eu}_2\text{L}_3$  which is fast and efficient only under a strict set of conditions.

### Introduction

The synthesis of supramolecular edifices is a fascinating area of current research in chemistry.<sup>1–11</sup> Metal template strategies, using the coordination of d- metals to oligopolydentate ligands, lead to homopolymetallic helicates,<sup>12–16</sup> ladder,<sup>17</sup> grids,<sup>18</sup> rings,<sup>19</sup>

cages,<sup>20,21</sup> and knots.<sup>22,23</sup> The peculiar photophysics of the lanthanides have aroused the development of efficient luminescent sensors with new supramolecular topographies, mainly bimetallic triple-stranded helicates.<sup>24–29</sup> For bioanalytical applications,<sup>30</sup> the ligand conception is of utmost importance and the chemist has to: (i) take into account the high lability, the large coordination numbers and the low steric requirements of the lanthanide ions,<sup>31</sup> (ii) include multiple absorbing groups suitable for light-harvesting and energy transfers,<sup>32</sup> and (iii) build

<sup>†</sup> Laboratoire de Physico-Chimie Bioinorganique.

<sup>‡</sup> Department of Inorganic, Analytical and Applied Chemistry.

<sup>§</sup> Laboratoire de Spectrométrie de Masse Bioorganique.

- (1) Lehn, J. M. *Supramolecular Chemistry: Concepts and Perspectives*; VCH: Weinheim, 1995; Chapter 9, p 139.
- (2) Lehn, J. M. *Proc. Natl. Acad. Sci. U.S.A.* **2002**, *99*, 4763–4768.
- (3) Constable, E. C. *Comprehensive Supramolecular Chemistry*; Sauvage, J. P., Hosseini, M. W., Eds.; Elsevier: Oxford, 1996; Vol. 9, Chapter 6, p 213.
- (4) Chambron, J. C.; Dietrich-Buchecker, C. O.; Sauvage, J. P. *Comprehensive Supramolecular Chemistry*; Sauvage, J. P., Hosseini, M. W., Eds.; Elsevier: Oxford, 1996; Vol. 9, Chapter 2, p 43.
- (5) Caulder, D. L.; Brückner, C.; Powers, R. E.; König, S.; Parac, T. N.; Leary, J. A.; Raymond, K. N. *J. Am. Chem. Soc.* **2001**, *123*, 8923–8938.
- (6) Davis, A. V.; Yeh, R. M.; Raymond, K. N. *Proc. Natl. Acad. Sci., U.S.A.* **2002**, *99*, 4793–4796.
- (7) Albrecht, M. *Chem. Rev.* **2001**, *101*, 3457–3497.
- (8) Albrecht, M.; Blau, O.; Fröhlich, R. *Proc. Natl. Acad. Sci., U.S.A.* **2002**, *99*, 4867–4872.
- (9) Kubota, Y.; Sakamoto, S.; Yamaguchi, K.; Fujita, M. *Proc. Natl. Acad. Sci., U.S.A.* **2002**, *99*, 4854–4856.
- (10) Kuehl, C. J.; Kryshchenko, Y. K.; Radhakrishnan, U.; Seidel, S. R.; Huang, S. D.; Stang, P. J. *Proc. Natl. Acad. Sci., U.S.A.* **2002**, *99*, 4932–4936.
- (11) Aoki, S.; Zülkefeli, M.; Shiro, M.; Kimura, E. *Proc. Natl. Acad. Sci., U.S.A.* **2002**, *99*, 4894–4899.
- (12) Fatin-Rouge, N.; Blanc, S.; Pfeil, A.; Rigault, A.; Albrecht-Gary, A. M.; Lehn, J. M. *Helv. Chim. Acta* **2001**, *84*, 1694–1711.
- (13) Fatin-Rouge, N.; Blanc, S.; Leize, E.; Van Dorsselaer, A.; Baret, P.; Pierre, J. L.; Albrecht-Gary, A. M. *Inorg. Chem.* **2000**, *39*, 5771–5778.
- (14) Rapenne, G.; Sauvage, J. P.; Patterson, B. T.; Richard, K. F. *Chem. Commun.* **1999**, 1853–1854.
- (15) Blanc, S.; Yakirevitch, P.; Leize, E.; Meyer, M.; Libman, J.; Van Dorsselaer, A.; Albrecht-Gary, A. M.; Shanzer, A. *J. Am. Chem. Soc.* **1997**, *119*, 4934–4944.
- (16) Bocquet, B.; Bernardinelli, G.; Ouali, N.; Floquet, S.; Renaud, F.; Hopfgartner, G.; Piguet, C. *Chem. Commun.* **2002**, 930–931.

- (17) Baxter, P. N. W.; Hanan, G. S.; Lehn, J. M. *Chem. Commun.* **1996**, 2019–2020.
- (18) Garcia, A. M.; Romero-Salguero, F. J.; Bassani, D. M.; Lehn, J. M.; Baum, G.; Fenske, D. *Chem. Eur. J.* **1999**, *5*, 1803–1808.
- (19) Hasenknopf, B.; Lehn, J. M.; Boumediene, N.; Dupont-Gervais, A.; Van Dorsselaer, A.; Kneisel, B.; Fenske, D. *J. Am. Chem. Soc.* **1997**, *119*, 10 956–10 962.
- (20) Machado, V. G.; Baxter, P. N. W.; Lehn, J. M. *J. Braz. Chem. Soc.* **2001**, *12*, 431–462.
- (21) Baxter, P. N. W.; Lehn, J. M.; Kneisel, B. O.; Baum, G.; Fenske, D. *Chem. Eur. J.* **1999**, *5*, 113–120.
- (22) Meyer, M.; Albrecht-Gary, A. M.; Dietrich-Buchecker, C. O.; Sauvage, J. P. *J. Am. Chem. Soc.* **1997**, *119*, 4599–4607.
- (23) Amabilino, D. B.; Stoddart, J. F. *Chem. Rev.* **1995**, *95*, 2725–2828.
- (24) Constable, E. C. *Tetrahedron* **1992**, *48*, 10 013–10 059.
- (25) Piguet, C.; Bernardinelli, G.; Hopfgartner, G. *Chem. Rev.* **1997**, *97*, 2005–2062.
- (26) Piguet, C.; Bünzli, J. C.; Bernardinelli, G.; Bochet, C. G.; Froidevaux, P. *J. Chem. Soc., Dalton Trans.* **1995**, 83–97.
- (27) Iglesias, C. P.; Elhabiri, M.; Hollenstein, M.; Bünzli, J. C.; Piguet, C. *J. Chem. Soc., Dalton Trans.* **2000**, 2031–2043.
- (28) Elhabiri, M.; Scopelliti, R.; Bünzli, J. C.; Piguet, C. *J. Am. Chem. Soc.* **1999**, *121*, 10 747–10 762.
- (29) Bünzli, J. C.; Piguet, C. *Chem. Rev.* **2002**, *102*, 1897–1928.
- (30) Desreux, J. F. *Lanthanide Probes in Life, Chemical and Earth Sciences: Theory and Practice*; Bünzli, J. C., Choppin, G. R., Eds.; Elsevier: Amsterdam, 1989.
- (31) Bünzli, J. C. *Rare Earths*; Saez, R., Caro, P., Eds.; Complutense: Madrid, 1998; p 223.
- (32) Bünzli, J. C.; Froidevaux, P.; Piguet, C. *New J. Chem.* **1995**, *19*, 661–668.

up thermodynamically stable and kinetically inert complexes. Among the numerous applications of the lanthanide compounds,<sup>30</sup> the replacement of radio-analytical assays, the sensing of various organic molecules, the chemical labeling of DNA or the specific cleavage of RNA, the production of new phosphors and the design of MRI contrast agents can be mentioned.<sup>33</sup> The characterization of bimetallic triple-stranded helicates by crystallography,<sup>27,28,34–37</sup> NMR,<sup>37,38</sup> mass spectrometry,<sup>39–41</sup> electrochemistry,<sup>42</sup> spectrophotometry, and potentiometry<sup>12,13,15,25,43,44</sup> has pointed out the main structural features involved in the formation of a helical architecture. The nature of the binding sites and of the cations imposes the number of strands. The length and the flexibility of the spacers between the metal coordination moieties also play an important role. They should be flexible enough to allow the ligand to bind strongly to the metal ion, and rigid enough to limit the number of conformations and favor interstrand over intrastrand binding. Finally, helicity implies that all metal centers must have the same helix direction and the same configuration at the metal centers.<sup>12,45</sup> If this key information was provided at equilibrium, then the kinetic parameters involved in the complexation mechanism have been rarely investigated for d-block helicates,<sup>12,13</sup> and are still unknown for f-block elements. The high potential of applications of the lanthanide helicates in chemical, biochemical and medical domains,<sup>46</sup> increases the interest of thermodynamic and kinetic studies of these compounds.

We report here the europium(III) coordination properties of the bis[1-methyl-2-(6'-[1''-(3,5-dimethoxybenzyl)benzimidazol-2''-yl]pyridin-2'-yl)benzimidazol-5-yl]methane (**L**), which corresponds to a strand containing two tridentate bis(benzimidazolyl)pyridine units (Figure 1a).<sup>47,48</sup>

The X-ray crystal structure<sup>47</sup> displays the helicoidal arrangement of the triple-stranded bimetallic complex  $\text{Eu}_2\text{L}_3$ . Three strands **L** are wrapped around the helical axis defined by the two lanthanide cations (Figure 1b). In each site, europium(III) is 9-coordinated by the 6 N atoms of the benzimidazole units and by the 3 N atoms of the pyridine groups respectively, in a slightly distorted tricapped trigonal prism geometry.

Speciation studies on the europium(III) complexes formed with **L** were carried out, while the self-assembly mechanism

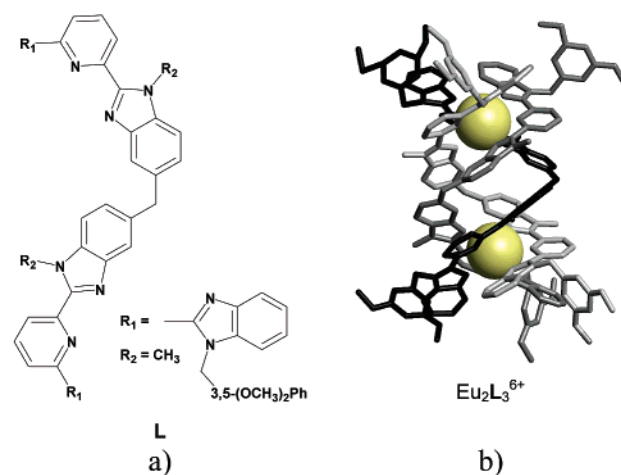


**Figure 1.** (a) Chemical formula of **L** and (b) view of the molecular structure of  $[\text{Eu}_2\text{L}_3]^{6+}$  perpendicular to the pseudo-3-fold axis.<sup>47,48</sup>

of  $\text{Eu}_2\text{L}_3$  was established using kinetic methods. These data obtained by ESMS, absorption spectrophotometry, and fast kinetic techniques, contribute to the understanding of the coordination chemistry of lanthanide complexes in order to prepare supramolecular precursors for functional devices.<sup>29,49</sup>

## Experimental Section

Ligand **L** ( $\text{C}_{59}\text{H}_{50}\text{N}_{10}\text{O}_4 \cdot 2\text{H}_2\text{O}$ ) and europium(III) perchlorate ( $\text{Eu}(\text{ClO}_4)_3 \cdot n\text{H}_2\text{O}$ ) were prepared according to literature procedures.<sup>48</sup> Stock solutions were prepared in pure acetonitrile (Fluka, 99.5% for spectroscopy) under argon atmosphere. The complete dissolution of **L** was obtained with the help of ultrasonic bath and its concentration ( $10^{-3}$  M) was calculated by weight. Stock europium(III) solutions were titrated by EDTA (Merck, Titriplex III,  $10^{-3}$  M) and xylenol orange (Merck) as indicator.<sup>50</sup> Solid samples of  $[\text{Eu}_2\text{L}_3](\text{ClO}_4)_6 \cdot 2\text{H}_2\text{O}$  were also solubilized in acetonitrile for mass spectrometric and spectrophotometric measurements. Charges have been omitted for the sake of clarity. **CAUTION! Although we have experienced no problems in handling perchlorate compounds, these salts combined with organic ligands are potentially explosive and should be handled in small quantities and with adequate precautions.**<sup>51,52</sup>

**Electrospray Mass Spectrometry.** Mass spectrometric measurements were carried out on a VG BioQ triple quadrupole with a mass to charge ( $m/z$ ) range of 4000 (Micromass Altrincham, UK) in the positive mode. The ES interface was heated to 60 °C. The sampling cone voltage ( $V_c$ ) was 30 V. The calibration was performed using multiprotonated ions from horse myoglobin. The resolution was about 600 at  $m/z = 1000$  (with a valley of 10%) and then average masses were measured. Scanning was performed from  $m/z = 200$  to 2400. The data system was operated as a multichannel analyzer, and several scans were summed to obtain the final spectrum. Solutions containing ligand **L** ( $0.4\text{--}5.0 \times 10^{-3}$  M) and 0.00, 0.02, 0.07, 0.50, 0.87, and 10.00 equivs of europium(III) were injected into the mass spectrometer source with a syringe pump (Harvard type 55 1111, Harvard Apparatus Inc., South Natick, MA) at a flow rate of 4  $\mu\text{L}/\text{min}$ . Additional mass spectra were recorded in the positive mode on a HP 1100 mass spectrometer (Agilent Technologies, Palo Alto, CA, formerly Hewlett-Packard Company Analytical Products Group). Scanning was performed from  $m/z = 200$  to 2400 and the sampling cone voltage ( $V_c$ ) was set at 55 V. Solutions containing ligand **L** and 1.00 equivalent of europium(III) as well as solutions prepared by dissolution of solid samples of

- (33) Piguet, C.; Bünzli, J. C. G. *Chimia* **1998**, *52*, 579–584.  
 (34) Lehn, J. M.; Rigault, A.; Siegel, J.; Harrowfield, J.; Chevrier, B.; Moras, D. *Proc. Natl. Acad. Sci., U.S.A.* **1987**, *84*, 2565–2569.  
 (35) Rigault, S.; Piguet, C.; Bernardinelli, G.; Hopfgartner, G. *Angew. Chem., Int. Ed. Engl.* **1998**, *37*, 169–172.  
 (36) Piguet, C.; Hopfgartner, G.; Bocquet, B.; Schaad, O.; Williams, A. F. *J. Am. Chem. Soc.* **1994**, *116*, 9092–9102.  
 (37) André, N.; Scopelliti, R.; Hopfgartner, G.; Piguet, C.; Bünzli, J. C. *Chem. Commun.* **2002**, 214–215.  
 (38) Meyer, M.; Kersting, B.; Powers, R. E.; Raymond, K. N. *Inorg. Chem.* **1997**, *36*, 5179–5191.  
 (39) Jaquinod, M.; Leize, E.; Potier, N.; Albrecht, A. M.; Shanzer, A.; Van Dorsselaer, A. *Tetrahedron Lett.* **1993**, *34*, 2771–2774.  
 (40) Hopfgartner, G.; Piguet, C.; Henion, J. D. *J. Am. Soc. Mass Spectrom.* **1994**, *5*, 748–756.  
 (41) Hopfgartner, G.; Piguet, C.; Henion, J. D.; Williams, A. F. *Helv. Chim. Acta* **1993**, *76*, 1759–1766.  
 (42) Greenwald, M.; Eassa, M.; Katz, E.; Willner, I.; Cohen, Y. *J. Electroanal. Chem.* **1997**, *434*, 77–82.  
 (43) Piguet, C.; Bernardinelli, G.; Bocquet, B.; Quattropani, A.; Williams, A. F. *J. Am. Chem. Soc.* **1992**, *114*, 7440–7451.  
 (44) Petoud, S.; Bünzli, J. C.; Renaud, F.; Piguet, C.; Schenk, K. J.; Hopfgartner, G. *Inorg. Chem.* **1997**, *36*, 5750–5760.  
 (45) Albrecht, M. *Chem. Eur. J.* **2000**, *6*, 3485–3489.  
 (46) Kumar, K.; Tweedle, M. F. *Pure Appl. Chem.* **1993**, *65*, 515–520.  
 (47) Bernardinelli, B.; Piguet, C.; Williams, A. F. *Angew. Chem., Int. Ed. Engl.* **1992**, *31*, 1622–1624.  
 (48) Piguet, C.; Bünzli, J. C.; Bernardinelli, G.; Hopfgartner, G.; Williams, A. F. *J. Am. Chem. Soc.* **1993**, *115*, 8197–8206.

- (49) Piguet, C.; Bünzli, J. C. *Chem. Soc. Rev.* **1999**, *28*, 347–358.  
 (50) *Méthodes d'Analyses Complexométriques avec les Titriplex*, E. Merck, Darmstadt.  
 (51) Wolsey, W. C. *J. Chem. Educ.* **1978**, *55*, A355.  
 (52) Raymond, K. N. *Chem. Eng. News* **1983**, *61*, 4.

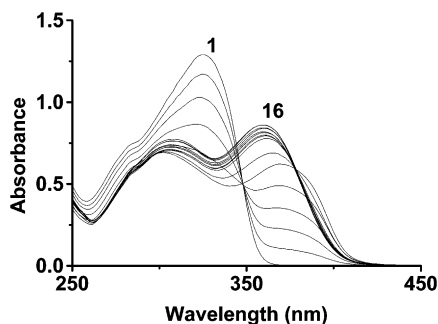


**Figure 2.** Spectrophotometric titration of **L** by europium(III). Solvent: acetonitrile;  $T = 25.0(1) ^\circ\text{C}$ ;  $l = 0.2 \text{ cm}$ ;  $[\text{L}]_{\text{tot}} = 9.64 \times 10^{-5} \text{ M}$ ; spectra 1–16:  $[\text{Eu}]_{\text{tot}} \times 10^4 \text{ M} = 0.00; 0.13; 0.25; 0.38; 0.51; 0.64; 0.76; 0.89; 1.02; 1.15; 1.27; 1.91; 2.54; 3.82; 5.09; 6.36$ .

$\text{Eu}_2\text{L}_3$  were injected into the mass spectrometer source with a syringe pump (Harvard type PHD 2000) at a flow rate of  $2 \mu\text{L}/\text{min}$ .

**Absorption Spectrophotometry.** The batch titration of **L** with europium(III) were undertaken in 5 mL flasks. Ligand concentration was fixed and the  $[\text{Eu}]_{\text{tot}}/[\text{L}]_{\text{tot}}$  ratio was varying between 0.13 and 6.60. The stability of the solutions was carefully checked and the corresponding UV–vis spectra were recorded on a Kontron Uvikon 941 spectrophotometer using Hellma quartz optical cells (1 or 0.2 cm). A spectrophotometric titration of **L** ( $[\text{L}]_{\text{tot}} = 9.64 \times 10^{-5} \text{ M}$ ;  $0.13 < [\text{Eu}]_{\text{tot}}/[\text{L}]_{\text{tot}} < 6.60$ ) is presented in Figure 2.

The spectrophotometric data were processed with both the Letagrop–Spefo and Specfit programs, which adjust the stability constants and the corresponding extinction coefficients of the species formed at equilibrium. Letagrop–Spefo<sup>53–55</sup> uses the Newton–Raphson algorithm to solve mass balance equations and a pit-mapping method to minimize the errors and determine the best values of the parameters. Specfit<sup>56–59</sup> uses factor analysis to reduce the absorbance matrix and to extract the eigenvalues prior to the multiwavelength fit of the reduced data set according to the Marquardt algorithm.<sup>60,61</sup> Distribution curves of the various species were calculated using the Haltafall program.<sup>62</sup>

**Kinetics.** The formation process of the triple-stranded bimetallic europium(III) helicate involves both slow and rapid steps. The kinetics were investigated using either an Applied Photophysics stopped-flow spectrophotometer SX-18MV or a Kontron Uvikon 941 spectrophotometer for fast and slow steps, respectively. The temperature was maintained at  $25.0(1) ^\circ\text{C}$  by the flow of a Lauda thermostat. Pseudo-first-order conditions with respect to europium(III) or to **L** were used ( $[\text{L}]_{\text{tot}} = 1.00 \times 10^{-5} \text{ M}$ ;  $1.06 \times 10^{-4} \text{ M} < [\text{Eu}]_{\text{tot}} < 1.00 \times 10^{-3} \text{ M}$  or  $[\text{Eu}]_{\text{tot}} = 5.15 \times 10^{-6} \text{ M}$ ;  $5.00 \times 10^{-5} \text{ M} < [\text{L}]_{\text{tot}} < 5.00 \times 10^{-4} \text{ M}$ ). The reaction was followed at 375 nm with a quartz optical cell of 1 cm. Data were processed with the Biokine software,<sup>63</sup> which fits up to three exponential functions to the experimental curves with the Simplex algorithm<sup>64</sup> after initialization with the Padé–Laplace method.<sup>65</sup> Time-resolved absorption spectra were also collected on an Applied Photophysics stopped-flow equipped with a diode array detector

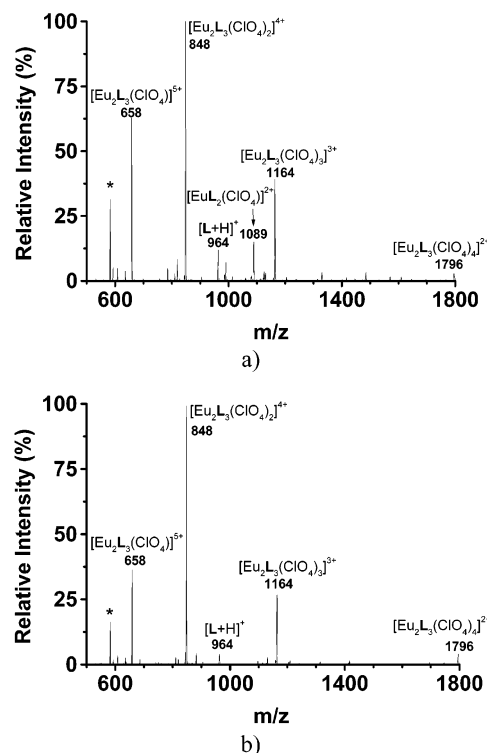


**Figure 3.** Electropray mass spectra of europium(III) complexes with **L**.  $V_c = 30 \text{ V}$ ; positive mode; solvent: acetonitrile. (a)  $[\text{L}]_{\text{tot}} = 1.00 \times 10^{-3} \text{ M}$ ,  $[\text{Eu}]_{\text{tot}} = 5.00 \times 10^{-4} \text{ M}$ ,  $[\text{Eu}]_{\text{tot}}/[\text{L}]_{\text{tot}} = 0.50$ ; (b)  $[\text{L}]_{\text{tot}} = 8.00 \times 10^{-4} \text{ M}$ ,  $[\text{Eu}]_{\text{tot}} = 7.01 \times 10^{-4} \text{ M}$ ,  $[\text{Eu}]_{\text{tot}}/[\text{L}]_{\text{tot}} = 0.87$ ; \* = impurities coming from solvent.

between 300 and 450 nm. Rate constants and extinction coefficients were adjusted to the multiwavelength data sets by nonlinear least-squares analysis with the Specfit software.<sup>56–59</sup> Variations of the pseudo-first-order rate constants with the analytical concentrations of reagents were fitted using commercial programs (Enzfitter,<sup>66</sup> Origin 5.0<sup>67</sup>).

## Results

**Electrospray Mass Spectra.** Electropray mass spectra were recorded in acetonitrile at various metal-to-ligand ratios (Figure 3 and Figure S1). The ionization of **L** was mainly obtained by the addition of protons and sodium ions. The mass spectrometric study showed the formation of three major europium(III) complexes, one monometallic species with two ligands ( $\text{EuL}_2$ ) and two bimetallic complexes with two and three ligands respectively ( $\text{Eu}_2\text{L}_2$ ,  $\text{Eu}_2\text{L}_3$ ). The ESMS spectra of solutions ( $4.90 \times 10^{-5} \text{ M} - 1.96 \times 10^{-6} \text{ M}$ ) with a precise  $3\text{L}/2\text{Eu}$  stoichiometry, which were prepared by dissolution in acetonitrile of solid samples  $\text{Eu}_2\text{L}_3$ , confirmed the presence of these three major species (Figure S1a). No significant fragmentation was observed under our experimental conditions. The peaks of the triple-stranded helicate dominate the spectra even in the presence of excess of europium(III) because unsaturated lanthanide complexes, where solvent molecules are coordinated to Ln(III) cation, are known to possess large solvation energies and weak ESMS responses.<sup>68</sup>

**Thermodynamics and Spectrophotometry.** The best fit<sup>53–59</sup> of the spectrophotometric titration (Figure 2) was obtained with

(53) Sillen, L. G. *Acta Chem. Scand.* **1964**, *18*, 1085–1098.  
 (54) Sillen, L. G.; Warnqvist, B. *Ark. Kemi.* **1968**, *31*, 377–390.  
 (55) Havel, J. *Pure Appl. Chem.* **1972**, *34*, 370–388.  
 (56) Gampp, H.; Maeder, M.; Meyer, C. J.; Zuberbühler, A. D. *Talanta* **1985**, *32*, 95–101.  
 (57) Rossoti, F. J. C.; Rossoti, H. S.; Whewell, R. J. *J. Inorg. Nucl. Chem.* **1971**, *33*, 2051–2065.  
 (58) Gampp, H.; Maeder, M.; Meyer, C. J.; Zuberbühler, A. D. *Talanta* **1985**, *32*, 257–264.  
 (59) Gampp, H.; Maeder, M.; Meyer, C. J.; Zuberbühler, A. D. *Talanta* **1986**, *33*, 943–951.  
 (60) Marquardt, D. W. *J. Soc. Indust. Appl. Math.* **1963**, *11*, 431–441.  
 (61) Maeder, M.; Zuberbühler, A. D. *Anal. Chem.* **1990**, *62*, 2220–2224.  
 (62) Ingri, N.; Kakolowicz, W.; Sillen, L. G.; Warnqvist, B. *Talanta* **1967**, *14*, 1261–1286.  
 (63) Bio-Logic Company, Ed. Bio-Logic Company, Echirrolles, **1991**.  
 (64) Nelder, J. A.; Mead, R. *Comput. J.* **1965**, *7*, 308–313.  
 (65) Yeremian, E.; Claverie, P. *Nature* **1987**, *326*, 169–174.

(66) Leatherbarrow, J. in *Enzfitter*; Biosoft Ed.: Cambridge, 1987.

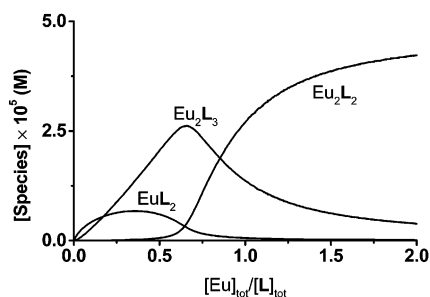
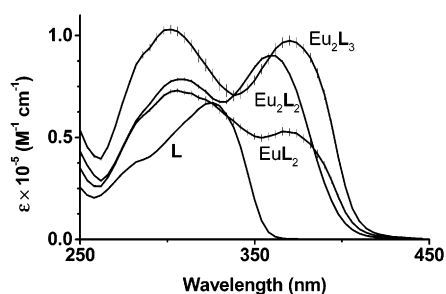
(67) Microcal Software, USA.

(68) Pignat, C.; Bünzli, J. C.; Bernardinelli, G.; Hopfgartner, G.; Petoud, S.; Schaad, O. *J. Am. Chem. Soc.* **1996**, *118*, 6681–6697.

**Table 1.** Global Stability Constants of Europium(III) Complexes with L<sup>a</sup>

$2\text{Eu} + 2\text{L} \rightleftharpoons \text{Eu}_2\text{L}_2$	$\log \beta_{\text{Eu}_2\text{L}_2} = 18.1(3)$
$2\text{Eu} + 3\text{L} \rightleftharpoons \text{Eu}_2\text{L}_3$	$\log \beta_{\text{Eu}_2\text{L}_3} = 24.3(4)$
$\text{Eu} + 2\text{L} \rightleftharpoons \text{EuL}_2$	$\log \beta_{\text{EuL}_2} = 11.6(3)$

<sup>a</sup> Solvent: acetonitrile;  $T = 25.0(1)^\circ\text{C}$ . Estimated errors  $\pm 3\sigma$ .

**Figure 4.** Distribution curves of europium(III) complexes with L versus  $[\text{Eu}]_{\text{tot}}$ . The stability constants are given in Table 1. Solvent: acetonitrile;  $T = 25.0^\circ\text{C}$ ;  $[\text{L}]_{\text{tot}} = 9.64 \times 10^{-5}\text{ M}$ .**Figure 5.** Electronic spectra of europium(III) complexes with L. Solvent: acetonitrile;  $T = 25.0^\circ\text{C}$ .

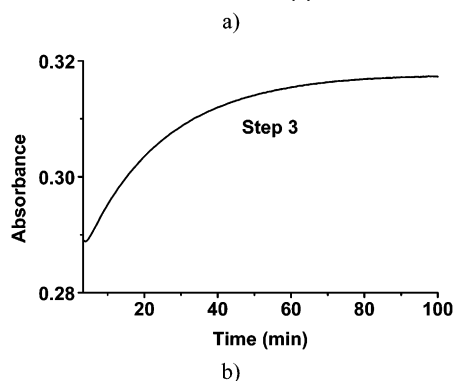
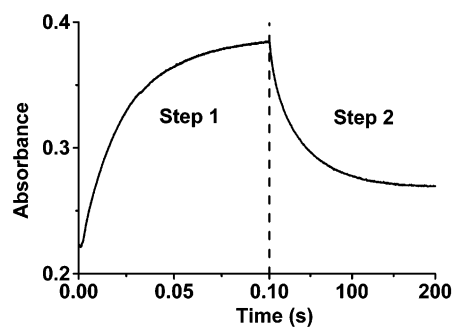
the three complexes previously observed by ESMS. The values of the global stability constants calculated for  $\text{EuL}_2$ ,  $\text{Eu}_2\text{L}_2$ , and  $\text{Eu}_2\text{L}_3$  are given in Table 1.

Using the  $\beta$  values presented in Table 1, we were able to calculate<sup>62</sup> the distribution diagram (Figure 4) of the europium(III) complexes formed with L under the experimental conditions of the spectrophotometric titration (Figure 2).

Moreover the electronic spectra of  $\text{EuL}_2$ ,  $\text{Eu}_2\text{L}_2$ , and  $\text{Eu}_2\text{L}_3$  (Figure 5) clearly show that the coordination of europium(III) induces a split of the ligand absorption band at 326 nm in two bands on either side of the maximum of L.

The absorption spectra recorded after dissolution of solid  $\text{Eu}_2\text{L}_3$  are in good agreement with the stability constants (Table 1) and with the extinction coefficients (Figure 5) of the three complexes observed by ESMS (Figure 3), as presented in Figure S2.

**Formation Kinetics in Excess of Europium(III).** The formation process of the europium(III) complexes was first investigated in excess of europium(III) with respect to L. Three exponential signals versus time were recorded at 375 nm. The use of a stopped-flow spectrophotometer was necessary to record the two first steps, while the slowest step was followed on a classical spectrophotometer. The total spectrophotometric amplitude measured versus time is in excellent agreement with the signal expected from the measurements at equilibrium. The fastest step could be easily extrapolated, taking into account 3 ms for the dead-time of the fast mixing device. This result shows that there is no additional step, which might be lost during the

**Figure 6.** Variation of the absorption versus time for the formation of europium(III) complexes with L in excess of  $[\text{Eu}]_{\text{tot}}$ . Solvent: acetonitrile;  $T = 25.0(1)^\circ\text{C}$ ;  $[\text{L}]_{\text{tot}} = 1.00 \times 10^{-5}\text{ M}$ ;  $[\text{Eu}]_{\text{tot}} = 1.86 \times 10^{-4}\text{ M}$ ;  $l = 1\text{ cm}$ ;  $\lambda = 375\text{ nm}$ . (a) Stopped-flow spectrophotometry; (b) absorption spectrophotometry.**Table 2.** Variation of the Pseudo-First-Order Rate Constants for the Formation of Europium(III) Complexes with L versus  $[\text{Eu}]_{\text{tot}}$ <sup>a</sup>

$[\text{Eu}]_{\text{tot}} \times 10^4\text{ (M)}$	$k_{1,\text{obs}}\text{ (s}^{-1}\text{)}$	$k_{2,\text{obs}} \times 10^2\text{ (s}^{-1}\text{)}$	$k_{3,\text{obs}} \times 10^2\text{ (s}^{-1}\text{)}$
1.06	15.1(6)	2.6(1)	0.66(5)
1.34	22.8(5)	1.98(6)	
1.57	35(1)	2.17(7)	0.78(7)
1.86	44(3)	2.23(7)	0.58(5)
2.55	80(16)	1.21(1)	
3.00	139(9)		1.6(1)
4.00	174(9)	1.07(3)	1.1(1)
5.00	217(9)	1.00(1)	
7.50		0.896(9)	
10.00		0.891(9)	

<sup>a</sup> Solvent: acetonitrile;  $T = 25.0(1)^\circ\text{C}$ ;  $[\text{L}]_{\text{tot}} = 1.00 \times 10^{-5}\text{ M}$ . Estimated errors  $\pm 3\sigma$ .

mixture of the reagents. Figure 6 displays an example of a kinetic curve. The different steps were successively denoted 1, 2, and 3.

The variation of the respective pseudo-first-order rate constants versus europium(III) in excess is given in Table 2.

A linear variation of  $k_{1,\text{obs}}$  versus  $[\text{Eu}]_{\text{tot}}$  is observed (Figure S3a). No significant ordinate at the origin was determined. For the fastest step, the following reaction 1 can be written as well as the corresponding rate law 2. The value of  $k_1$  is given in Table 3.



$$d[\text{EuL}]/dt = k_1 \times [\text{Eu}]_{\text{tot}} \times [\text{L}] \quad (2)$$

When  $[\text{Eu}]_{\text{tot}}$  increases, the pseudo-first-order rate constant  $k_{2,\text{obs}}$ , relative to the second rate-limiting step, decreases (Table 2). The variation of  $k_{2,\text{obs}}$  versus  $[\text{Eu}]_{\text{tot}}$  is given in Figure S3b. These

**Table 3.** Rate Constants and Thermodynamic Parameters Determined by Kinetic Studies for the Formation Mechanism of Europium(III) Complexes with **L**<sup>a</sup>

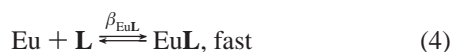
equilibrium	excess of Eu(III)	excess of <b>L</b>
$\text{Eu} + \text{L} \xrightleftharpoons[k_{-1}]{k_1} \text{EuL}$	$k_1 = 4.0(3) \times 10^5 \text{ M}^{-1} \text{ s}^{-1}$	$k_1 = 4.6(7) \times 10^5 \text{ M}^{-1} \text{ s}^{-1}$ $k_{-1} = 13(9) \text{ s}^{-1}$ $k_1/k_{-1} = 4(3) \times 10^4 \text{ M}^{-1}$
$\text{EuL} + \text{L} \xrightleftharpoons[k_{-2}]{k_2} \text{EuL}_2$	$k_2 = 1.2(2) \times 10^4 \text{ M}^{-1} \text{ s}^{-1}$ $k_{-2} = 6(2) \times 10^{-3} \text{ s}^{-1}$ $k_2/k_{-2} = 2.0(1) \times 10^6 \text{ M}^{-1}$ $\beta_{\text{EuL}} = 2(1) \times 10^5 \text{ M}^{-1}$	$k_2 = 6.0(2) \times 10^4 \text{ M}^{-1} \text{ s}^{-1}$
$\text{EuL}_2 + \text{Eu} \xrightleftharpoons[k_{-3}]{k_3} \text{Eu}_2\text{L}_2$		$k_3 = 2.2(4) \times 10^6 \text{ M}^{-1} \text{ s}^{-1}$ $k_{-3} = 0.17(1) \text{ s}^{-1}$ $k_3/k_{-3} = 1.3(2) \times 10^7 \text{ M}^{-1}$
$\text{Eu}_2\text{L}_2 + \text{L} \xrightleftharpoons[k_{-4}]{k_4} \text{Eu}_2\text{L}_3$	$k_{-4} = 1.0(2) \times 10^{-3} \text{ s}^{-1}$	$k_4 = 6.2(8) \times 10^3 \text{ M}^{-1} \text{ s}^{-1}$ $k_4/k_{-4} = 7(2) \times 10^5 \text{ M}^{-1}$

<sup>a</sup> Solvent: acetonitrile;  $T = 25.0$  °C. Calculated standard errors.

experimental data suggest that the binding of a second strand **L** to **EuL** takes place according to the following equilibrium



If we consider that equilibrium 4 is fast compared to eq 3, then



it is possible to write the following rate eq 5

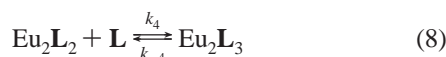
$$\frac{d[\text{EuL}_2]}{dt} = \frac{k_2 \times \beta_{\text{EuL}} \times [\text{Eu}]_{\text{tot}} \times ([\text{L}]_{\text{tot}} - 2[\text{EuL}_2])^2}{(1 + \beta_{\text{EuL}} \times [\text{Eu}]_{\text{tot}})^2} - k_{-2} \times [\text{EuL}_2] \quad (5)$$

Under our experimental conditions, the rate constant  $k_{2,\text{obs}}$  yields

$$k_{2,\text{obs}} = k_{-2} + \frac{4 \times k_2 \times \beta_{\text{EuL}} \times [\text{L}]_{\text{tot}} \times [\text{Eu}]_{\text{tot}}}{(1 + \beta_{\text{EuL}} \times [\text{Eu}]_{\text{tot}})^2} \quad (6)$$

The values of the rate constants  $k_2$  and  $k_{-2}$  and of the equilibrium constant  $\beta_{\text{EuL}}$  are given in Table 3.

A decrease of more than 1 order of magnitude is observed for the rate constant  $k_{3,\text{obs}}$  compared to  $k_{2,\text{obs}}$  (Table 2).  $k_{3,\text{obs}}$  does not significantly vary with  $[\text{Eu}]_{\text{tot}}$  (Figure S3c). These data suggest the rapid formation of  $\text{Eu}_2\text{L}_2$  followed by a slow binding of the third strand **L** leading to the bimetallic helicate in step 3 (Figure 6)



The corresponding rate law can be expressed by

$$d[\text{Eu}_2\text{L}_3]/dt = k_4 \times [\text{Eu}_2\text{L}_2] \times [\text{L}] - k_{-4} \times [\text{Eu}_2\text{L}_3] \quad (9)$$

If we assume that the three first successive equilibria are reached, then we can use the corresponding stability constants, solve a second degree equation from the mass balance equation

and then evaluate  $[\text{L}]$  using a first-order limited expansion of the square root considering that  $[\text{Eu}_2\text{L}_3]$  is small

$$[\text{L}] \approx \frac{[\text{L}]_{\text{tot}}}{1 + \beta_{\text{EuL}} \times [\text{Eu}]_{\text{tot}}} \quad (10)$$

Substituting  $[\text{L}]$  into the rate law leads to the following expression

$$\frac{d[\text{Eu}_2\text{L}_3]}{dt} = \frac{k_4 \times \beta_{\text{Eu}_2\text{L}_2} \times [\text{Eu}]_{\text{tot}}^2 \times [\text{L}]_{\text{tot}}^3}{(1 + \beta_{\text{EuL}} \times [\text{Eu}]_{\text{tot}})^3} - k_{-4} \times [\text{Eu}_2\text{L}_3] \quad (11)$$

Under our experimental conditions, we could deduce that  $k_{3,\text{obs}}$  could be approximated to  $k_{-4}$  (Table 3).

Moreover, to gain information on the fast steps of the formation process of **L** europium(III) complexes, in the presence of metal in excess, we recorded time-resolved spectra, using a stopped-flow spectrophotometer equipped with diode arrays (Figure S4). Factor analysis of the entire spectrophotometric data set confirmed the presence of three major absorbing species (**L**, **EuL** and  $\text{Eu}_2\text{L}_2$ ). A satisfactory least-squares fit of the apparent rate constants and electronic spectra could be obtained in agreement with the previous scheme of successive reaction steps.<sup>56–59</sup>

**Formation Kinetics in Excess of **L**.** Four exponential rate-limiting signals were recorded versus time at 375 nm (Figure S5). These steps which are in the seconds range, were determined using a stopped-flow spectrophotometer. Taking into account the dead-time (3 ms) of the fast mixing device and an injection artifact due to acetonitrile, we extrapolated the fastest exponential signal to an absorbance value which was in agreement with the spectrophotometric data determined at equilibrium. The different steps were successively denoted 1, 2, 3, and 4 (Figure S5). The corresponding pseudo-first-order constants  $k'_{\text{obs}}$  ( $\text{s}^{-1}$ ) determined at various **L** concentrations in excess are given in Table S1. The variation of these pseudo-first-order rate constants is presented in Figure 7.

We observe a linear variation, with a significant ordinate at the origin, of  $k'_{1,\text{obs}}$  versus  $[\text{L}]_{\text{tot}}$  (Figure 7a) in agreement with the following equilibrium



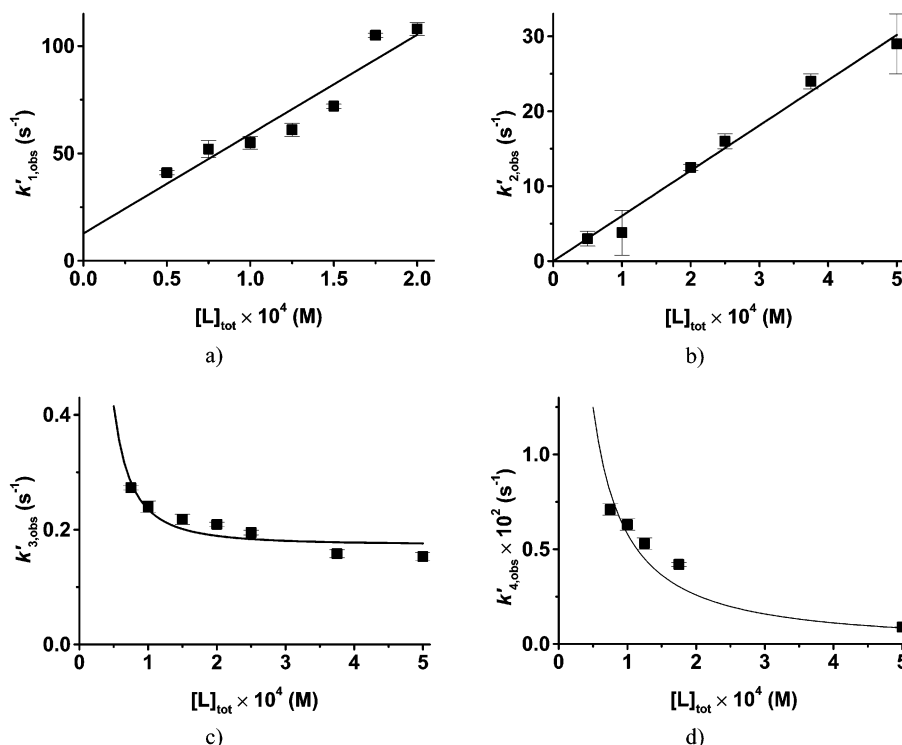


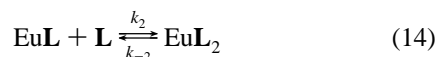
**Figure 7.** Variation of the (a) first, (b) second, (c) third, and (d) fourth pseudo-first-order rate constants for the formation of europium(III) complexes with **L** versus  $[\mathbf{L}]_{\text{tot}}$ . Solvent: acetonitrile;  $T = 25.0$  (1)°C.

The corresponding rate law is

$$d[\text{EuL}]/dt = k_1 \times [\text{Eu}] \times [\mathbf{L}]_{\text{tot}} - k_{-1} \times [\text{EuL}] \quad (13)$$

We deduced that  $k'_{1,\text{obs}} = k_1 \times [\mathbf{L}]_{\text{tot}} + k_{-1}$  and calculated the values of  $k_1$  and  $k_{-1}$  (Table 3).

The formation of  $\text{EuL}_2$  could explain the linear variation of  $k'_{2,\text{obs}}$  versus  $[\mathbf{L}]_{\text{tot}}$  (Figure 7b)

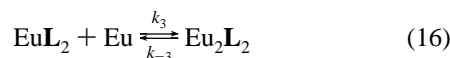


The rate of this reaction is expressed by eq 15 which leads to the determination of  $k_2$  (Table 3)

$$d[\text{EuL}_2]/dt = k_2 \times [\text{EuL}] \times [\mathbf{L}]_{\text{tot}} - k_{-2} \times [\text{EuL}_2] \quad (15)$$

We deduce that  $k'_{2,\text{obs}} = k_{-2} + (k_2 \times \beta_{\text{EuL}} \times [\mathbf{L}]_{\text{tot}}^2) / (1 + \beta_{\text{EuL}} \times [\mathbf{L}]_{\text{tot}})$ . The constant  $k_{-2}$  is not accessible under our experimental conditions and if  $1 \ll \beta_{\text{EuL}} \times [\mathbf{L}]_{\text{tot}}$ , we can write  $k'_{2,\text{obs}} = k_2 \times [\mathbf{L}]_{\text{tot}}$ . The linear regression of our data gives:  $k_2 = 6.0(2) \times 10^4 \text{ M}^{-1} \text{ s}^{-1}$  (Table 3).

The decrease of  $k'_{3,\text{obs}}$  versus  $[\mathbf{L}]_{\text{tot}}$  (Figure 7c) could be attributed to the binding of a second europium(III) cation to the monometallic complex  $\text{EuL}_2$



The resolution of the following differential equation

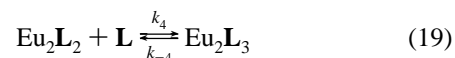
$$d[\text{Eu}_2\text{L}_2]/dt = k_3 \times [\text{EuL}_2] \times [\text{Eu}] - k_{-3} \times [\text{Eu}_2\text{L}_2] \quad (17)$$

leads, under our experimental conditions, to the reduced expression 18

$$k'_{3,\text{obs}} = k_{-3} + \frac{4 \times k_3 \times \beta_{\text{EuL}_2} \times [\mathbf{L}]_{\text{tot}} \times [\text{Eu}]_{\text{tot}}}{(1 + \beta_{\text{EuL}} \times [\mathbf{L}]_{\text{tot}} + \beta_{\text{EuL}_2} \times [\mathbf{L}]_{\text{tot}}^2)^2} \quad (18)$$

The values of the rate constants  $k_3$  and  $k_{-3}$  are given in Table 3.

We give in Figure 7d the variation of the fourth apparent rate constant with  $[\mathbf{L}]_{\text{tot}}$ . We propose the following reaction for this step



The rate law corresponding to equilibrium 19 is expressed by

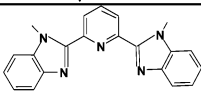
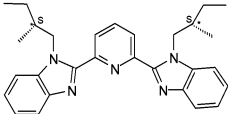
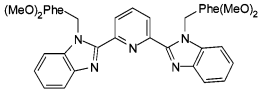
$$d[\text{Eu}_2\text{L}_3]/dt = k_4 \times [\text{Eu}_2\text{L}_2] \times [\text{Eu}] - k_{-4} \times [\text{Eu}_2\text{L}_3] \quad (20)$$

Under our experimental conditions, we can use the steady-state approximation for  $\text{Eu}_2\text{L}_2$  to solve this differential equation. We write  $d[\text{Eu}_2\text{L}_2]/dt = 0$  and deduce the expression for  $k'_{4,\text{obs}}$

$$k'_{4,\text{obs}} = \frac{4 \times k_3 \times k_4 \times \beta_{\text{EuL}_2} \times [\mathbf{L}]_{\text{tot}}^3 \times [\text{Eu}]_{\text{tot}}}{(k_4 \times [\mathbf{L}]_{\text{tot}} + k_{-3}) \times (1 + \beta_{\text{EuL}} \times [\mathbf{L}]_{\text{tot}} + \beta_{\text{EuL}_2} \times [\mathbf{L}]_{\text{tot}}^2)^2} + \frac{k_{-3} \times k_{-4}}{k_4 \times [\mathbf{L}]_{\text{tot}} + k_{-3}} \quad (21)$$

Our experimental data were fitted using the rate constants ( $k_3$ ,  $k_{-3}$ , and  $k_{-4}$ ) and the stability constants ( $\beta_{\text{EuL}}$  and  $\beta_{\text{EuL}_2}$ )

**Table 4.** Stepwise Stability Constants of Europium(III) Complexes Formed with **L** and Benzimidazole Derivatives<sup>a</sup>

$\text{Eu} + \text{L} \rightleftharpoons \text{EuL}$	$\log K_{\text{EuL}} = 4.6(3)^b$
$\text{EuL} + \text{L} \rightleftharpoons \text{EuL}_2$	$\log K_{\text{EuL}_2} = 7.0(4)$
$\text{EuL}_2 + \text{Eu} \rightleftharpoons \text{Eu}_2\text{L}_2$	$\log K_{\text{Eu}_2\text{L}_2} = 6.5(4)$
$\text{Eu}_2\text{L}_2 + \text{L} \rightleftharpoons \text{Eu}_2\text{L}_3$	$\log K_{\text{Eu}_2\text{L}_3} = 6.2(5)$
	$\log K_{\text{Eu}(\text{L}^1)} = 9.0(2)$
<b>L<sup>1c</sup></b>	$\log K_{\text{Eu}(\text{L}^1)_2} = 6.7(3)$
	$\log K_{\text{Eu}(\text{L}^1)_3} = 6.9(4)$
	$\log K_{\text{Eu}(\text{L}^2)} = 8.2(2)$
<b>L<sup>2d</sup></b>	$\log K_{\text{Eu}(\text{L}^2)_2} = 5.9(3)$
	$\log K_{\text{Eu}(\text{L}^2)_3} = 4.0(5)$
	$\log K_{\text{Sm}(\text{L}^3)_2} = 5.5(1)$
<b>L<sup>3c,e</sup></b>	$\log K_{\text{Sm}(\text{L}^3)_3} = 3.6(1)$
	$\log K_{\text{Gd}(\text{L}^3)_2} = 4.8(1)$
	$\log K_{\text{Gd}(\text{L}^3)_3} = 3.2(1)$

<sup>a</sup> Solvent: acetonitrile;  $T = 25.0(1)^\circ\text{C}$ . <sup>b</sup> From kinetic data. <sup>c</sup> From ref 44. <sup>d</sup> From ref 69. <sup>e</sup> Not measured for europium(III),  $\log K_{\text{EuL}^3}$  was fixed ( $\geq 9$ ). For the sake of simplicity, charges have been omitted.

which are presented in Table 3. They led to the value of  $k_4 = 6.2(8) \times 10^2 \text{ M}^{-1} \text{ s}^{-1}$  (Table 3).

## Discussion

The goal of this study is to examine the self-assembly process of the bimetallic triple-helical complex  $\text{Eu}_2\text{L}_3$ . Thermodynamic and kinetic data will allow us to point out the main structural and chemical features involved in the  $\text{Eu} - \text{L}$  system.

**Characterization of Europium(III) Complexes with **L**.** Depending on the  $[\text{Eu}]_{\text{tot}}/[\text{L}]_{\text{tot}}$  ratio, three europium(III) complexes,  $\text{EuL}_2$ ,  $\text{Eu}_2\text{L}_2$ , and  $\text{Eu}_2\text{L}_3$  were characterized in acetonitrile by ESMS (Figure 3, Figure S1) and by absorption spectrophotometry (Figure 5). Moreover, the stability constant of  $\text{EuL}$  and its electronic spectrum were deduced from kinetic data (Table 4, Figure S4b).

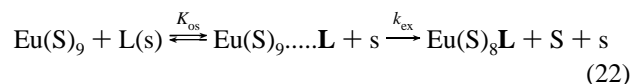
The most surprising result is the low stability of  $\text{EuL}$ ,  $K_{\text{EuL}}$  being 3–4 orders of magnitude lower than  $K_{\text{EuL}^1}$  and  $K_{\text{EuL}^2}$  in the same solvent. By contrast, the successive stability constant of  $\text{EuL}_2$  is significantly higher than the corresponding parameters determined for the monotopic analogues **L**<sup>1</sup>, **L**<sup>2</sup>, and **L**<sup>3</sup> under identical experimental conditions. The global stability constant of the bimetallic double-stranded complex  $\text{Eu}_2\text{L}_2$  is equal to 18.1(3), which is in agreement with the values determined elsewhere for similar systems.<sup>27,30</sup> The stability constant of  $\text{Eu}_2\text{L}_3$  ( $\log \beta_{\text{Eu}_2\text{L}_3} = 24.3(4)$ ) is about 2–4 orders of magnitude higher than the value estimated to  $20 < \log$

$\beta_{\text{Eu}_2\text{L}_3} < 22$  in a previously published work,<sup>48</sup> but it is close to the values determined for analogous helicates.<sup>27,70</sup> This difference can be traced back to the oversimplified model used to fit the data and to partial thermodynamic equilibrium of the sample's solutions in the preliminary study. The distribution diagram (Figure 4) shows that the bimetallic helicate  $\text{Eu}_2\text{L}_3$  is the major complex under our experimental conditions ( $[\text{L}]_{\text{tot}} \approx 10^{-4} \text{ M}$ ) in a large range of stoichiometry  $[\text{Eu}]_{\text{tot}}/[\text{L}]_{\text{tot}}$  between 0.2 and 0.8. These results indicate that, when europium(III) is not in excess with respect to **L**, the self-assembly of  $\text{Eu}_2\text{L}_3$  exhibits positive cooperativity<sup>71</sup> as already mentioned for trimetallic double-stranded helicates with  $\text{Cu}(\text{I})$ <sup>12,72</sup> and  $\text{Ag}(\text{I})$ <sup>73</sup> and triple-stranded diferric complexes.<sup>15</sup>

To discuss the spectrophotometric properties of the europium(III) complexes with **L**, we have collected in Table S2 spectrophotometric data available for europium(III) complexes formed with various bis(benzimidazolyl)pyridine derivatives in acetonitrile.<sup>26,69,74,75</sup> Our ligand **L** displays a broad band in the UV region centered at 326 nm, which is assigned to  $\pi_1 \rightarrow \pi^*$  transitions.<sup>26,76</sup> Upon complexation with europium(III), this band splits into two distinct components ( $\pi_1^a \rightarrow \pi^*$  and  $\pi_1^b \rightarrow \pi^*$ ) as previously described for **L**<sup>1</sup> – **L**<sup>7</sup> complexes (Table S2).<sup>48,77</sup> The complexation of two europium(III) cations approximately leads to twice higher molar absorption coefficients for the  $\pi_1^a \rightarrow \pi^*$  and  $\pi_1^b \rightarrow \pi^*$  transitions with respect to monometallic complexes  $[\text{Eu}(\text{L}^i)_n]$  ( $i = 1-7$ ;  $n = 2, 3$ ). Similar band splits are observed for  $\text{EuL}_2$ ,  $\text{Eu}_2\text{L}_2$ , and  $\text{Eu}_2\text{L}_3$  and suggest a similar coordination of the tridentate segments to europium(III) cation<sup>47</sup> in these three species.

**Self-Assembly Process of Eu(III) Helicate.** A four steps formation process (Table 3) was evidenced for the formation of the triple-stranded helicate  $\text{Eu}_2\text{L}_3$ .

Step 1 leads to the formation of  $\text{EuL}$ . We will compare the  $\text{EuL}$  formation rate with that expected from a dissociative Eigen–Wilkins<sup>78</sup> mechanism



The fast formation of the outer-sphere complex, which involves desolvation of the ligand, is characterized by an equilibrium constant  $K_{\text{os}}$ , which may be evaluated by the *Fuoss* relationship.<sup>79</sup> The bimolecular rate constant for the formation of  $\text{EuL}$  can be expressed by the following equation

$$k_{\text{f}} = K_{\text{os}} \times k_{\text{ex}} = 0.16 \times k_{\text{ex}} \quad (23)$$

If the solvent exchange rate constant on europium(III) in acetonitrile is of the same order of magnitude as values

- (69) Muller, G.; Bünzli, J. C. G.; Schenk, K. J.; Piguet, C.; Hopfgartner, G. *Inorg. Chem.* **2001**, *40*, 2642–2651.  
 (70) Martin, N.; Bünzli, J. C.; McKee, V.; Piguet, C.; Hopfgartner, G. *Inorg. Chem.* **1998**, *37*, 577–589.  
 (71) Lindsey, J. S. *New J. Chem.* **1991**, *15*, 153–180.  
 (72) Pfeil, A.; Lehn, J. M. *J. Chem. Soc., Chem. Commun.* **1992**, 838–840.  
 (73) Garrett, T. M.; Koert, U.; Lehn, J. M. *J. Phys. Org. Chem.* **1992**, *5*, 529–532.  
 (74) Piguet, C.; Williams, A. F.; Bernardinelli, G.; Bünzli, J. C. *Inorg. Chem.* **1993**, *32*, 4139–4149.  
 (75) Piguet, C.; Williams, A. F.; Bernardinelli, G.; Moret, E.; Bünzli, J. C. *Helv. Chim. Acta* **1992**, *75*, 1697–1717.  
 (76) Nakamoto, K. *J. Phys. Chem.* **1960**, *64*, 1420–1425.  
 (77) Piguet, C.; Bocquet, B.; Müller, E.; Williams, A. F. *Helv. Chim. Acta* **1989**, *72*, 323–327.  
 (78) Eigen, M.; Wilkins, R. G. *Adv. Chem. Ser.* **1965**, *49*, 55–67.  
 (79) Fuoss, R. M. *J. Am. Chem. Soc.* **1958**, *80*, 5059–5061.

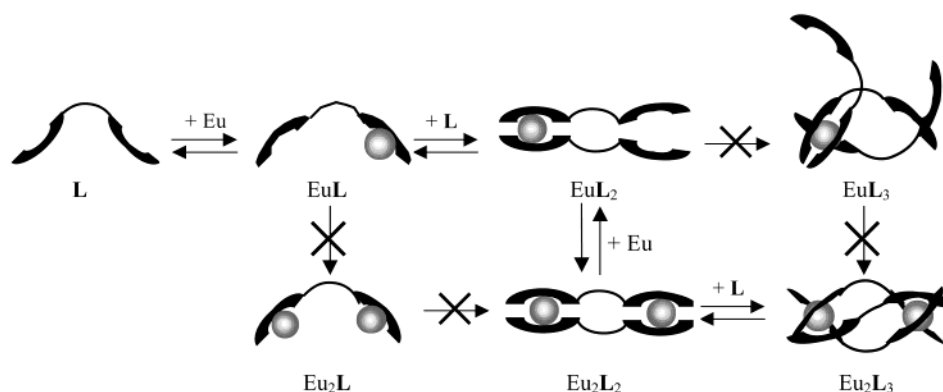


**Figure 8.** Schematic representation of the proposed mechanism.

determined in water<sup>80</sup> and DMF<sup>81</sup> ( $\sim 10^8$ – $10^9$  s<sup>-1</sup>), then  $k_f$  is equal to  $\sim 10^7$ – $10^8$  M<sup>-1</sup> s<sup>-1</sup>. Our rate constant  $k_1$  ( $\sim 4 \times 10^5$  M<sup>-1</sup> s<sup>-1</sup>) is about 2 orders of magnitude lower. The rate-limiting step obviously does not correspond to the simple desolvation of europium(III). This result strongly suggests that complexation of Eu by **L** could involve concerted structural changes which result in slower kinetics.<sup>82–87</sup> In solution and in the solid state, in the absence of coordinating cations, it has been shown that the monotopic tridentate receptors **L**<sup>1</sup> – **L**<sup>7</sup> (Table S2) adopt a trans–trans conformation in order to minimize dipole moment and reduce the steric hindrance when bulky substituents are introduced.<sup>88</sup> As well as the monotopic ligands, the ditopic strands exhibit *transoid* conformation in solution as demonstrated by <sup>1</sup>H-NMR spectroscopy (NOE effect).<sup>27,28,44,70</sup> During the coordination process, a rotation about the biaryl bond, already observed for copper(I) complexation with poly(2,2'-bipyridine) ligands<sup>12,89</sup> and transition metal complexes formed with tridentate terpyridine ligands,<sup>90</sup> should occur to allow multiple ion coordination. Moreover, a comparison of the stability constants of the kinetic species Eu**L** with thermodynamic species Eu**L**<sup>1</sup> and Eu**L**<sup>2</sup> examined in the same solvent shows that presence of bulky substituents strongly reduces the stability of Eu**L**. Nevertheless, stability constant of Eu**L** is higher than those reported for bidentate ligands such as bipyridine or phenanthroline, suggesting a partial or distorted binding of the tridentate units of **L**.<sup>91,92</sup>

The second step is related to the addition of a second strand. We have to mention that the approach of a second europium(III) cation will be precluded by strong Coulombic repulsions,

whereas the coordination of a neutral ligand will be more favorable leading to a less solvated Eu**L**<sub>2</sub> complex. Furthermore, the approach of a second ligand strand is favored, because the first europium is probably not completely encapsulated by the first ligand. The value of the dissociation constant ( $k_{-1} = 13$  s<sup>-1</sup>) indeed indicated a rather labile Eu**L** species. We observe that the bimolecular rate constant  $k_2$  ( $k_2 \approx 6 \times 10^4$  M<sup>-1</sup> s<sup>-1</sup>) is 10 times lower than the former one ( $k_1 \approx 4 \times 10^5$  M<sup>-1</sup> s<sup>-1</sup>) in agreement with steric effects due to the approach of a second ligand. The dissociation rate constant of Eu**L**<sub>2</sub> ( $k_{-2} \approx 6 \times 10^{-3}$  s<sup>-1</sup>), which is 4 orders of magnitude lower than that observed for Eu**L**, confirms stabilizing dipole and/or dispersion interactions in the double-stranded species.<sup>74,90</sup>

The third step is assigned to the complexation of the second europium(III) cation. We observe that the coordination of the second cation to Eu**L**<sub>2</sub> ( $k_3 = 2.2 \times 10^6$  M<sup>-1</sup> s<sup>-1</sup>) is about 1 order of magnitude faster than the coordination of the first europium(III) cation, but 2–3 orders of magnitude lower than the solvent exchange rate constant on europium(III) ( $10^8$ – $10^9$  s<sup>-1</sup>). Considering the charge of the Eu**L**<sub>2</sub><sup>3+</sup> acceptor and that of the entering cation, a dissociative *Eigen–Wilkins*<sup>78</sup> mechanism may account for our data ( $K_{os} = 10^{-3}$  M<sup>-1</sup>,  $k_3 \approx 10^6$  M<sup>-1</sup> s<sup>-1</sup>). Our results show that the binding of europium(III) to Eu**L**<sub>2</sub> does not involve any structural rearrangements, but is mainly governed by electrostatic repulsions and desolvation of the entering cation. This could be also in line with the non statistical distribution of heterobimetallic triple-stranded helicates observed by <sup>1</sup>H NMR spectroscopy showing that when one ion is smaller than europium(III), the organization of the second coordination site is more favorable for a second lanthanide ion of similar size.<sup>37,48</sup> We suggest that Eu**L**<sub>2</sub> could adopt in solution a side-by-side arrangement as already reported for the X-ray crystallographic structure of unsaturated double-stranded bimetallic complex formed with a similar strand.<sup>25,70</sup>

The final “braiding”<sup>93</sup> of the third strand on the side-by-side Eu**L**<sub>2</sub> leads to the formation of the bimetallic triple-stranded helicate. Highly distorted coordination geometries, as observed in our previous work on the self-assembly process of tricuprous double helicates,<sup>12</sup> and non helicoidal structure, as for Eu**L**<sub>2</sub> in this work, constitute reactive key intermediates for the supramolecular arrangement processes. Increase of the steric hindrance and more strained structures contribute to slow the

(80) Cossy, C.; Helm, L.; Merbach, A. E. *Inorg. Chem.* **1988**, *27*, 1973–1979.

(81) Helm, L.; Merbach, A. E. *Coord. Chem. Rev.* **1999**, *187*, 151–181.

(82) Shi, Y.; Eyring, E. M.; van Eldik, R. *J. Chem. Soc., Dalton Trans.* **1998**, 3565–3576.

(83) Kumar, K.; Jin, T.; Wang, X.; Desreux, J. F.; Tweedle, M. F. *Inorg. Chem.* **1994**, *33*, 3823–3829.

(84) Choi, K. Y.; Kim, D. W.; Hong, C. P. *Polyhedron* **1995**, *14*, 1299–1306.

(85) Powell, D. H.; Favre, M.; Graeppl, N.; Dhuhghaill, O. M. N.; Pubanz, D.; Merbach, A. E. *J. Alloys Compound* **1995**, *225*, 246–252.

(86) Rothermel, G. L.; Rizkalla, E. N.; Choppin, G. R. *Inorg. Chim. Acta* **1997**, *262*, 133–138.

(87) Chang, C. A.; Liu, Y. L.; Chen, C. Y.; Chou, X. M. *Inorg. Chem.* **2001**, *40*, 3448–3455.

(88) Nozary, H.; Pigué, C.; Rivera, J. P.; Tissot, P.; Bernardinelli, G.; Vulliermet, N.; Weber, J.; Bünzli, J. C. *Inorg. Chem.* **2000**, *39*, 5286–5298.

(89) Annunziata, R.; Benaglia, M.; Famulari, A.; Raimond, L. *Magn. Res. Chem.* **2001**, *39*, 341–354.

(90) Priimov, G. U.; Moore, P.; Helm, L.; Merbach, A. E. *Inorg. React. Mech.* **2001**, *3*, 1–23.

(91) Hancock, R. D.; Jackson, G.; Evers, A. *J. Chem. Soc., Dalton Trans.* **1979**, *9*, 1384–1387.

(92) Pyatnitskii, I.; Makarcheuk, T.; Gavrilova, E. *Zh. Neorg. Khim.* **1984**, *29*, 2141–2143.

(93) Charbonnière, L. J.; Williams, A. F.; Frey, A.; Merbach, A. E.; Kamalprija, P.; Schaad, O. *J. Am. Chem. Soc.* **1997**, *119*, 2488–2496.



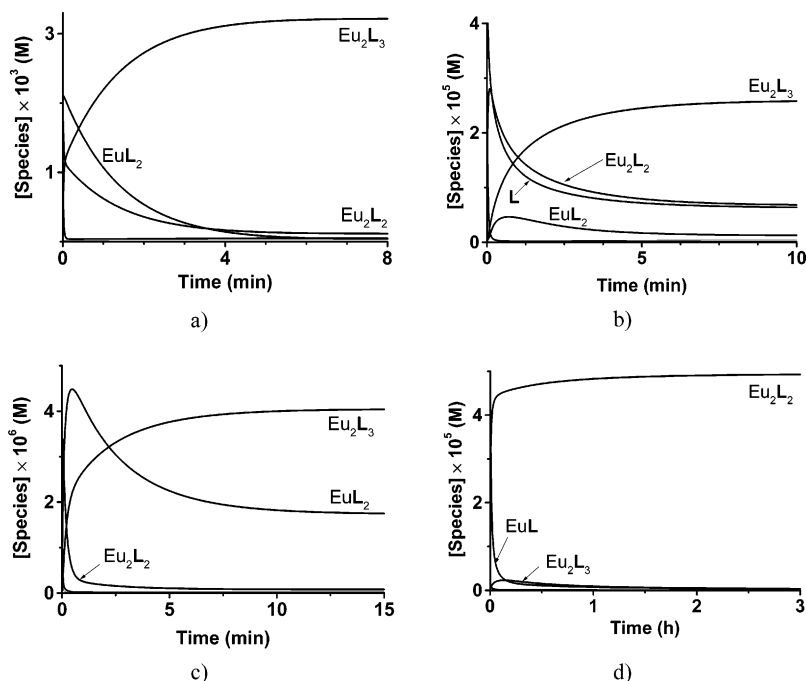


**Figure 9.** Simulation of the concentration variation of the different europium(III) complexes formed with **L** versus time using the kinetic constants given in Table 3. Solvent: acetonitrile;  $T = 25.0\text{ }^{\circ}\text{C}$ . (a)  $[\text{L}]_{\text{tot}} = 10^{-2}\text{ M}$ ,  $[\text{Eu}]_{\text{tot}}/[\text{L}]_{\text{tot}} = 0.67$ ; (b)  $[\text{L}]_{\text{tot}} = 10^{-4}\text{ M}$ ,  $[\text{Eu}]_{\text{tot}}/[\text{L}]_{\text{tot}} = 0.67$ ; (c)  $[\text{L}]_{\text{tot}} = 10^{-4}\text{ M}$ ,  $[\text{Eu}]_{\text{tot}}/[\text{L}]_{\text{tot}} = 0.1$ ; (d)  $[\text{L}]_{\text{tot}} = 10^{-4}\text{ M}$ ,  $[\text{Eu}]_{\text{tot}}/[\text{L}]_{\text{tot}} = 10$ .

addition of the third strand to  $\text{Eu}_2\text{L}_2$  ( $k_4 = 6.2 \times 10^2\text{ M}^{-1}\text{ s}^{-1}$ ). The respective values of  $k_{-2}$  ( $6.0 \times 10^{-3}\text{ s}^{-1}$ ) and  $k_{-4}$  ( $1.0 \times 10^{-3}\text{ s}^{-1}$ ) show that the successive “braiding” process significantly enhances the inertness of the corresponding complexes  $\text{EuL}_2$  and  $\text{Eu}_2\text{L}_3$ , whereas the “keystone” addition of the second europium(III) cation leads to the labile species  $\text{Eu}_2\text{L}_2$  ( $k_{-3} = 0.17\text{ s}^{-1}$ ). Therefore, it has been observed that the wrapping and assembly mechanism of three ligand strands around the two metallic centers is essentially governed by ion–dipole interactions while aromatic  $\pi$ – $\pi$  stacking seemingly played no role neither in the final helical edifice<sup>70</sup> nor in the intermediate complexes.

It is significant that we observe a good agreement, within experimental errors, between kinetics ( $\beta_{\text{EuL}_2} \approx 2 \times 10^{11}\text{ M}^{-2}$ ;  $\beta_{\text{Eu}_2\text{L}_2} = 0.7 \times 10^{18}\text{ M}^{-3}$ ;  $\beta_{\text{Eu}_2\text{L}_3} = 1.2 \times 10^{24}\text{ M}^{-4}$ ) and thermodynamics ( $\beta_{\text{EuL}_2} = 4 \times 10^{11}\text{ M}^{-2}$ ;  $\beta_{\text{Eu}_2\text{L}_2} = 1.3 \times 10^{18}\text{ M}^{-3}$ ;  $\beta_{\text{Eu}_2\text{L}_3} = 2 \times 10^{24}\text{ M}^{-4}$ ) which supports our mechanistic interpretation schematically illustrated in Figure 8.

Figure 9 presents the kinetic curves, which were simulated under various europium(III) and ligand **L** concentrations. For  $[\text{L}]_{\text{tot}} = 10^{-4}\text{ M}$ , we notice that the equilibrium is reached in the time range of minutes for the stoichiometry of the helicate (Figure 9b) as well as in excess of **L** (Figure 9c). Nevertheless, hours are necessary to achieve the equilibration in excess of europium(III) (Figure 9d). Higher concentrations of **L** ( $[\text{L}]_{\text{tot}} = 10^{-2}\text{ M}$ ) strongly favor the dinuclear triple-stranded helicate (Figure 9a). This is also an interesting illustration of the thermodynamic and kinetic behavior of  $\text{Eu}_2\text{L}_3$ , which is not significantly formed in excess of cation, but which is rapidly formed in excess of ligand. Figure 9a and b clearly show that increased concentrations of **L** and stoichiometry conditions induce a fast self-assembly of  $\text{Eu}_2\text{L}_3$ , which becomes the only product of the reaction.

## Conclusion

The present study has allowed us to better understand the mechanistic processes occurring during formation of the triple-stranded helicate  $\text{Eu}_2\text{L}_3$ . The formation of  $\text{EuL}$  strongly suggests slow and concerted conformation changes of strand **L**. The structure of  $\text{EuL}$  prevents a fast addition of the second europium(III) cation and favors the “braiding” of a second strand. The addition of a second europium(III) cation in a “keystone” process leads to a labile side-by-side  $\text{Eu}_2\text{L}_2$  species, which allows the “braiding” of the third strand in the final bimetallic triple-stranded helicate  $\text{Eu}_2\text{L}_3$ . Interestingly, the  $\text{Eu}_2\text{L}_3$  formation is mainly governed by electrostatic interactions. The kinetic studies clearly demonstrate that the apparent “magic”, quantitative and fast, self-assembly of five partners ( $3\text{L}/2\text{ Eu}$ ) into the final helicate  $\text{Eu}_2\text{L}_3$  is only observed under strict stoichiometric conditions with high reagent concentrations. Deviations from these asymptotic conditions severely limit (and sometimes prevent) the formation of the target helicate: a crucial point which must be carefully considered when programming multicomponents self-assembly processes.

**Acknowledgment.** This work has been supported by the Centre National de la Recherche Scientifique, the Faculty of Chemistry, University Louis Pasteur, Strasbourg (France) and the Department of Inorganic, Analytical and Applied Chemistry, University of Geneva (Switzerland). J. H. thanks the European Community for granting him a Marie Curie fellowship. The authors thank R. Hueber for his skillful assistance in the ESMS measurements.

**Supporting Information Available:** Figures showing additional mass spectra (S1), comparison of calculated and experimental absorption spectra (S2), variation of the pseudo-

first-order rate constants ( $k_{1,obs}$ ,  $k_{2,obs}$ , and  $k_{3,obs}$ ) in excess of europium(III) (S3), time-resolved absorption spectra in excess of europium(III) (S4), formation kinetics in excess of **L** (S5) are given. Table (S1) with pseudo-first-order rate constants in excess of **L** and Table (S2) with absorption maxima of Eu(III)

complexes with **L** and bis(benzimidazolyl)pyridine derivatives are given. This material is available free of charge via the Internet at <http://pubs.acs.org>.

JA028861Q